



**HAL**  
open science

# Isolation of a dodecanuclear polyoxo cluster Nb<sub>12</sub>O<sub>21</sub> showing a rare case of five-fold coordinated niobium(V) centers with a square pyramidal geometry

Despoina Andriotou, Natacha Henry, Sylvain Duval, Christophe Volkringer, William E Shepard, Frederique Pourpoint, Thierry Loiseau

## ► To cite this version:

Despoina Andriotou, Natacha Henry, Sylvain Duval, Christophe Volkringer, William E Shepard, et al.. Isolation of a dodecanuclear polyoxo cluster Nb<sub>12</sub>O<sub>21</sub> showing a rare case of five-fold coordinated niobium(V) centers with a square pyramidal geometry. *European Journal of Inorganic Chemistry*, 2023, *European Journal of Inorganic Chemistry*, 26 (30), pp.e202300432. 10.1002/ejic.202300432 . hal-04272640

**HAL Id: hal-04272640**

**<https://hal.univ-lille.fr/hal-04272640>**

Submitted on 10 Nov 2023

**HAL** is a multi-disciplinary open access archive for the deposit and dissemination of scientific research documents, whether they are published or not. The documents may come from teaching and research institutions in France or abroad, or from public or private research centers.

L'archive ouverte pluridisciplinaire **HAL**, est destinée au dépôt et à la diffusion de documents scientifiques de niveau recherche, publiés ou non, émanant des établissements d'enseignement et de recherche français ou étrangers, des laboratoires publics ou privés.

**Isolation of a dodecanuclear polyoxo cluster {Nb<sub>12</sub>O<sub>21</sub>} showing a rare case of five-fold coordinated niobium(V) centers with a square pyramidal geometry**

**Dr. Despoina Andriotou,<sup>[a]</sup> Dr. Natacha Henry,<sup>[a]</sup> Dr. Sylvain Duval,<sup>\*[a]</sup> Prof. Christophe Volkringer,<sup>[a]</sup> Dr. William E. Shepard, Dr. Frédérique Pourpoint,<sup>[a]</sup> and Dr. Thierry Loiseau<sup>[a]</sup>**

*Contribution from*

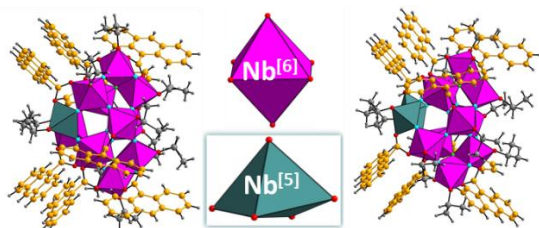
<sup>a</sup> *Unité de Catalyse et Chimie du Solide (UCCS) – UMR CNRS 8181, Université de Lille, Centrale Lille, Université d’Artois, F-59000 Lille, France.*

<sup>b</sup> *Univ. Lille, CNRS, INRAE, Centrale Lille, Univ. Artois, FR 2638 – IMEC – Institut Michel-Eugène Chevreul, Lille, 59000, France.*

<sup>c</sup> *Synchrotron SOLEIL, L’Orme des Merisiers, Saint Aubin BP48, F-91192, Gif sur Yvette, France).*

\* To whom correspondence should be addressed. E-mail: [sylvain.duval@univ-lille.fr](mailto:sylvain.duval@univ-lille.fr), Phone: (33) 3 20 43 41 22, Fax: (33) 3 20 43 48 95.

## Table of Content (TOC) Graphic



Isolation of two large dodecameric  $\{\text{Nb}_{12}\text{O}_{21}\}$  clusters in the same lattice was achieved by combination of  $\text{NbCl}_4 \cdot 2\text{THF}$  with anthracene-9-carboxylic acid. The clusters are constituted of octahedral niobium(V) centers associated with rarely seen square pyramidal niobium(V) cations.

**ABSTRACT:** The reactivity of the complexing anthracene-9-carboxylate ligand has been investigated with a niobium(IV) tetrachloride precursor ( $\text{NbCl}_4 \cdot 2\text{THF}$ ) in isopropanol solvent. This resulted in the crystallization of a molecular assembly containing two distinct  $\{\text{Nb}_{12}\text{O}_{21}\}$  cores surrounded by multiple isopropanolate and anthracenoate ligands. The compound is formulated  $[\text{Nb}_{12}(\mu_3\text{-O})_3(\mu\text{-O})_{18}(\text{C}_{15}\text{H}_9\text{O}_2)_8(\text{O}^i\text{Pr})_{10}] \cdot [\text{Nb}_{12}(\mu_3\text{-O})_2(\mu\text{-O})_{19}(\text{C}_{15}\text{H}_9\text{O}_2)_8(\text{O}^i\text{Pr})_{10}]$  illustrating the two different dodecameric oxo-clusters, for which the niobium(IV) precursor was oxidized in the niobium(V) state during the reactional process. The two distinct  $\{\text{Nb}_{12}\text{O}_{21}\}$  units mainly differs by the environment of the niobium centers, which exhibits unexpected five-fold coordination (square pyramid) for some of them, together with the classical six-fold coordination (octahedron) as usually found for niobium(V). In the crystallization process, the IR spectroscopy was used to analyze the esterification reaction occurring between the anthracene acid an isopropanolate ligands responsible of the production of water used in the oxo-condensation of the niobium centers.  $^{93}\text{Nb}$  Solid state NMR was tentatively used to assess the occurrence of the different niobium environments.

## Introduction

Niobium is a d-block transition metal that is still studied, mainly under the oxide form or as a doping element in other metals, for catalytic purpose.<sup>[1-6]</sup> It exists with several oxidation states, principally Nb(III), Nb(IV) or Nb(V), the latter being the most currently used. The main reason is the stability of the oxidation state +5 in comparison with the two other ones (+3, +4) which require specific handling environment. Few examples of clusters with carboxylates ligands have been described and shows nuclearities ranging from the monomer up to the hexamer with the 4+ oxidation state.<sup>[7-12]</sup> Under its oxidation stable Nb(V) state, it has long been used in molecular chemistry for the synthesis of polynuclear oxo-clusters. Two main approaches have efficiently been performed and have led to two categories of well-known molecular families. The first one belongs to the polyoxometalates field, where niobium is surrounded by oxo ligands and feature the presence of “yl” terminal oxygen atoms preventing or strongly limiting the formation of extended networks. Nevertheless, numerous molecular polyoxometallic compounds have been described through the years, and are perfectly well represented and described in the recent review of Zhao *et al.*<sup>[13]</sup> It is reported all the different architectures arising from the well-known  $[\text{Nb}_6\text{O}_{19}]^{8-}$  Lindqvist polyanion<sup>[14]</sup> up to the largest aggregate possessing 288 niobium centers.<sup>[15]</sup> Different strategies and classifications are used in the review to describe these molecular entities, generally based on isopolyoxoniobates or heteropolyoxoniobates, sometimes associated with heterometals allowing aggregation of complex molecular entities. The second family related to “hybrid poly-oxo clusters” consists of niobium centers surrounded by oxo-donor ligands from different organic ligands types (alkoxides,  $\text{R-O}^-$ , or carboxylates,  $\text{R-COO}^-$ ) with a total absence of terminal “yl” oxygen atoms existing in classical polyoxometalates. In addition, for these polynuclear hybrid oxo clusters, bridging oxygen atoms can be found in the molecular structure. As far as we know, these hybrids niobium compounds are systematically molecular association and, extended networks have yet to be discovered. In molecular chemistry of hybrid niobium clusters, commercial precursors can be found and can be described as discrete Nb-centered mononuclear unit,

precipitated by oxalic acid to give  $[A][NbO(C_2O_4)_2(H_2O)_2] \cdot xH_2O$  ( $A = NH_4^{+16,17}$  or  $Cs^{+18}$ ) or  $[A]_3[NbO(C_2O_4)_3] \cdot xH_2O$  ( $A = NH_4^{+19}$  or  $Rb^{+20}$ ) salts, which can be further associated using pyridine-based molecules (phenanthroline, bipyridine, etc...)<sup>[21]</sup> or divalent transition metals complexes with  $[Zn(bpy)]^{2+}$ ,<sup>[22]</sup>  $[Co(terpy)]^{2+}$ ,<sup>[23]</sup>  $[(Fe-Zn)(bpy)]^{2+}$ <sup>[24]</sup> ( $bpy = 2,2'$ -bipyridine,  $terpy = 2,2':6',2''$ -terpyridine) and rare-earth cations.<sup>[25]</sup> Other niobium oxalates have also been isolated in the presence of non-metallic divalent counter cations such as barium in  $[Ba_2(H_2O)_5][NbO(C_2O_4)_3][HC_2O_4] \cdot H_2O$ <sup>[26]</sup> or with peroxide groups.<sup>[19]</sup> Several peroxo niobium centers can also be found in a series of complexes involving citrate, tartrate, ethylenediaminetetraacetate (edta) and propylenediaminetetraacetate (pdta) ligands.<sup>[27-29]</sup> To isolate molecules with more than one niobium centers, monomeric pentachloride  $NbCl_5$  or dimeric alkoxide  $Nb_2(\mu-OR)_2(OR)_8$  niobium precursors have been used.  $NbCl_5$  reactivity was first studied using the benzoic acid ligand ( $HO_2C-C_6H_5$ ) and leads to the formation of two molecular dinuclear compounds, in which the niobium centers are bridged through the carboxylate arm of the monotopic benzoate molecules. In one case, the dimer  $[Nb_2O(O_2C-C_6H_5)_2Cl_6]$ <sup>[30]</sup> possesses one additional  $\mu_2$ -oxo group bridging the two niobium centers, whereas it does not exist in the second molecule  $[Nb_2(OEt)_4(O_2C-C_6H_5)_2Cl_4]$ .<sup>[31]</sup> Other monotopic benzoate derivatives ( $O_2C-R$  where  $R = FC_6H_4$ ,  $p-ClC_6H_4$ ,  $p-IC_6H_4$ ,  $p-MeC_6H_4$ ) with modifications on the aromatic ring are also mentioned in the work of Brown *et al.*<sup>[31-33]</sup> In this work, addition of ethanol as a solvent in the initial solution led to the exchange of some chloride anions by ethoxy (OEt) groups, stabilizing the dimeric configuration without any central bridging  $\mu$ -oxo atom. A related dinuclear complex was also identified with completely fluorosubstituted benzoate linker ( $O_2C-C_6F_5$ ) in a purely chloride salt  $[Nb_2Cl_8(O_2C-C_6F_5)_2]$ .<sup>[32]</sup> The second synthetical pathway is using metal alkoxides precursors ( $M(OR)_n$ , where  $R = Me$  for methoxide, OEt for ethoxide, etc). This method has been more intensely studied, since these hybrid compounds are known for their utilization as precursors for the elaboration of ceramics<sup>[34-37]</sup> and the substitution by a bidentate ligand can contribute to the modification of its properties.<sup>[38-43]</sup> Regarding the chemistry of molecular niobium alkoxides, many coordination complexes have been identified with various monocarboxylic acids and different niobium nuclearities. For instance, identification of dinuclear niobium complex  $[Nb_2O(O_{Nep})_6(piv)_2]$  (where  $O_{Nep} = OCH_2CMe_3$  or neopentanoxy) in the presence of pivalic acid ( $Me_3C-CO_2H = Hpiv$ ) was performed. This dimer is related to another one,  $[Nb_2O(O_2C-C_6H_5)_2Cl_6]$ ,<sup>[30]</sup> synthesized from the halide precursor and possessing two carboxylate arms from two pivalate ligands and one bridging  $\mu$ -oxo group and chloride instead of neopentanoxy ligands. In the previous system, when using *tert*-butylacetic acid ( $Me_3C-CH_2-CO_2H = HtBAC$ ) instead of pivalic acid, a higher condensed coordination complex  $[Nb_4O_4(O_{Nep})_8(tBAC)_4]$  containing four niobium centers placed in a square configuration and connected to four  $\mu$ -oxo groups has been isolated. This tetramer can be seen as the combination of the two previously described dinuclear compounds  $[Nb_2O(O_{alkoxide})_3(carboxylate)_2]$  linked together by two additional  $\mu$ -oxo groups. Other research groups also come across this tetranuclear unit using other ligands. Hubert-Pfalzgraf *et al.* obtained the compound  $[Nb_4O_4(ac)_4(O^iPr)_8]$ <sup>[44]</sup> (with  $ac = acetate$ ) and  $[Nb_4O_4(MAA)_4(O^iPr)_8]$ <sup>[45]</sup> (with  $MAA = methacrylate$ ) starting from niobium isopropoxide. The use of niobium alkoxides is important for the formation of tetranuclear niobium coordination complexes. Indeed, the alkoxy groups, leaving as alcohols molecules

when a carboxylate arm complex niobium centers, are involved in an esterification process slowly generating water molecules leading to the creation of  $\mu$ -oxo-bridges between the niobium centers of the cluster. Other related compounds have been synthesized by using bis(hydroxymethyl)propionic acid ( $H_2BHMP$ ). In this system, the niobium dimers contain one  $\mu$ -oxo bridge and are interacting with both the carboxylate and hydroxy functions of the ligand.<sup>[46]</sup> This interaction generates through the BHMP ligand, a tetranuclear species  $[(BHMP)\{Nb_2O(OEt)_5\}_2]$ , without any additional  $\mu$ -oxo groups linking the niobium atoms. Such an association of niobium carboxylate from the alkoxide route is also illustrated in a mixed bismuth-niobium moiety,<sup>[47]</sup> which has been synthesized using salicylic acid (2-hydroxybenzoic acid) leading to a dinuclear  $[(Bi_2Nb_2O(OEt)_2(sal)_4(Hsal)_4)]$  or tetranuclear  $[(Bi_2Nb_4O_4(O^iPr)_4(sal)_4(Hsal)_3)]$  (with  $sal = O_2C-C_6H_4-2-O$ ;  $Hsal = O_2C-C_6H_4-2-OH$ ) coordination complexes. Increasing clusters nuclearity in molecular chemistry is always a challenge. Lately, coordination modes behavior of niobium and tantalum was studied using catecholate ligands.<sup>[48]</sup> To date, the largest poly-oxo cluster in niobium carboxylate chemistry has been identified from a solvothermal reaction of niobium ethoxide with pivalic acid in acetonitrile. It led to the formation of an hexadecaniobate cluster  $[Nb_{16}O_{28}(OEt)_{12}(piv)_{12}]$ .<sup>[49]</sup> In our recent work on this topic, we have used several aromatic monocarboxylic and polycarboxylic acid ligands to complex niobium(IV) tetrachloride and niobium(V) ethoxide precursors, successfully increasing the nuclearity of the niobium centers in the final compounds up to the formation of an octameric  $\{Nb_8O_{12}\}$  moieties.<sup>[50–52]</sup>

In this contribution, we report on the investigation of the reactivity of the anthracene-9-carboxylic acid ligand with niobium(IV) tetrachloride  $NbCl_4(THF)_2$  precursor as the niobium(IV) source. The reaction occurring in isopropanol solvent at 120°C leads to the formation of a molecular crystalline compound containing niobium(V) centers involved in two distinct  $\{Nb_{12}O_{21}\}$  cores. These two units are surrounded by isopropanolate and anthracenoate ligands  $[Nb_{12}(\mu_3-O)_3(\mu-O)_{18}(C_{15}H_9O_2)_8(O^iPr)_{10}] \cdot [Nb_{12}(\mu_3-O)_2(\mu-O)_{19}(C_{15}H_9O_2)_8(O^iPr)_{10}] \cdot \approx 7(HO^iPr)$  where the two distinct dodecamers are contained in the same crystal structure, but with different coordination environments for some niobium centers, which can be six-fold or five-fold oxo-surrounded. The compound was successfully characterized by single-crystal and powder X-ray diffraction and MAS  $^{93}Nb$  NMR spectroscopy and some insights in its formation behavior is given with the help of infrared spectroscopy.

## Results and discussion

### Structure Description

**Compound**  $[Nb_{12}(\mu_3-O)_3(\mu_2-O)_{18}(C_{15}H_9O_2)_8(O^iPr)_{10}] \cdot [Nb_{12}(\mu_3-O)_2(\mu_2-O)_{19}(C_{15}H_9O_2)_8(O^iPr)_{10}] \cdot \approx 7(HO^iPr)$

The crystal structure consists of two distinct neutral closely related molecular moieties, which contain twelve niobium(V) centers linked through oxo groups and bonded to anthracene-9-carboxylate and isopropanolate species, resulting in a  $\{Nb_{12}O_{21}\}$  core. They are named by the letter A for the entity  $[Nb_{12}(\mu_3-O)_3(\mu_2-O)_{18}(C_{15}H_9O_2)_8(O^iPr)_{10}]$  and letter B for the entity

[Nb<sub>12</sub>(μ<sub>3</sub>-O)<sub>2</sub>(μ<sub>2</sub>-O)<sub>19</sub>(C<sub>15</sub>H<sub>9</sub>O<sub>2</sub>)<sub>8</sub>(O<sup>i</sup>Pr)<sub>10</sub>], related to the two crystallographically independent motifs. For a better understanding of the complex arrangement of the niobium atoms, both dodecameric cores A and B can be viewed as the association of two hexameric sub-units {Nb<sub>6</sub>O<sub>x</sub>}.

For molecule A, a first sub-unit (named A1) is built up from six octahedrally-coordinated niobium centers (Figure 1-left). There are two sets of two octahedral polyhedra [NbO<sub>6</sub>] sharing an edge of one μ<sub>3</sub>-oxo and one μ<sub>2</sub>-oxo bridges, which inserts two others octahedral polyhedra [NbO<sub>6</sub>] sharing one μ<sub>2</sub>-oxo bridge. The three sets of niobium pairs are connected to each other either via three μ<sub>2</sub>-oxo groups and one μ<sub>3</sub>-oxo group, in order to generate a rectangular-like sub-unit {Nb<sub>6</sub>O<sub>8</sub>} (A1). For the second hexanuclear sub-unit (A2 – Figure 1-right), the arrangement of the Nb-centered polyhedra is similar, except that one of the two peripheral sets of niobium pairs is replaced by two niobium atoms sharing one μ<sub>2</sub>-oxo bridge (instead of an edge-sharing mode as found in sub-unit A1). Indeed, for this particular niobium pair, one of the metal centers (Nb11) is five-fold coordinated with a distorted square pyramidal geometry. It results in a second type of rectangular-like sub-unit {Nb<sub>6</sub>O<sub>7</sub>} (A2). It is observed slightly shorter Nb-O bond lengths for the five-fold coordinated Nb11 atoms, with Nb11-O<sub>μ<sub>2</sub></sub> distances in the range 1.847(5)-1.891(6) Å, one Nb11-O<sub>c</sub> (O<sub>c</sub> = carboxyl oxygen) distance of 2.153(6) Å and one Nb11-O<sub>Pr</sub> (O<sub>Pr</sub> = oxygen from isopropanolate) distance of 1.828(6) Å. In comparison with the other Nb-O bond lengths of the octahedrally niobium atoms (Table S1), it is found that the Nb-O<sub>Pr</sub> distance of the five-coordinated Nb11 atom is in the same range (≈ 1.86-1.83 Å). But the Nb-O<sub>c</sub> and Nb-O<sub>μ<sub>2</sub>/μ<sub>3</sub></sub> distances for Nb11, are in the lower values of the Nb-O ranges (≈ 2.14-2.24 Å and ≈ 1.80-2.41 Å, respectively) reported in the eleven six-fold coordinated niobium centers of the molecule A. For the sub-unit {Nb<sub>6</sub>O<sub>8</sub>} (A1), one notes one untypical long Nb6-O<sub>7μ<sub>3</sub></sub> distance of 2.409(5) Å, which strongly distorts the Nb6-centered octahedra environment. Such a geometrical distortion was sometimes reported in different niobium oxides, such as CaNb<sub>2</sub>O<sub>5</sub><sup>[53]</sup> (Rb,Cs)Sr<sub>2</sub>Nb<sub>3</sub>O<sub>10</sub><sup>[54]</sup> or LiNbUO<sub>6</sub><sup>[55]</sup> for instance. At the opposite, in the sub-unit {Nb<sub>6</sub>O<sub>7</sub>} (A2), the corresponding oxygen atom (O16 – see Figure 1-right) is much more remote with a Nb11⋯O16 distance of 3.036(7) Å, which excludes the octahedral geometry of the Nb11 atom. This subtle Nb-O distance variation is at the origin of the differentiation between the two hexanuclear sub-units A1 and A2, with the occurrence of one unique five-fold coordination for Nb11 atoms in sub-unit A2.

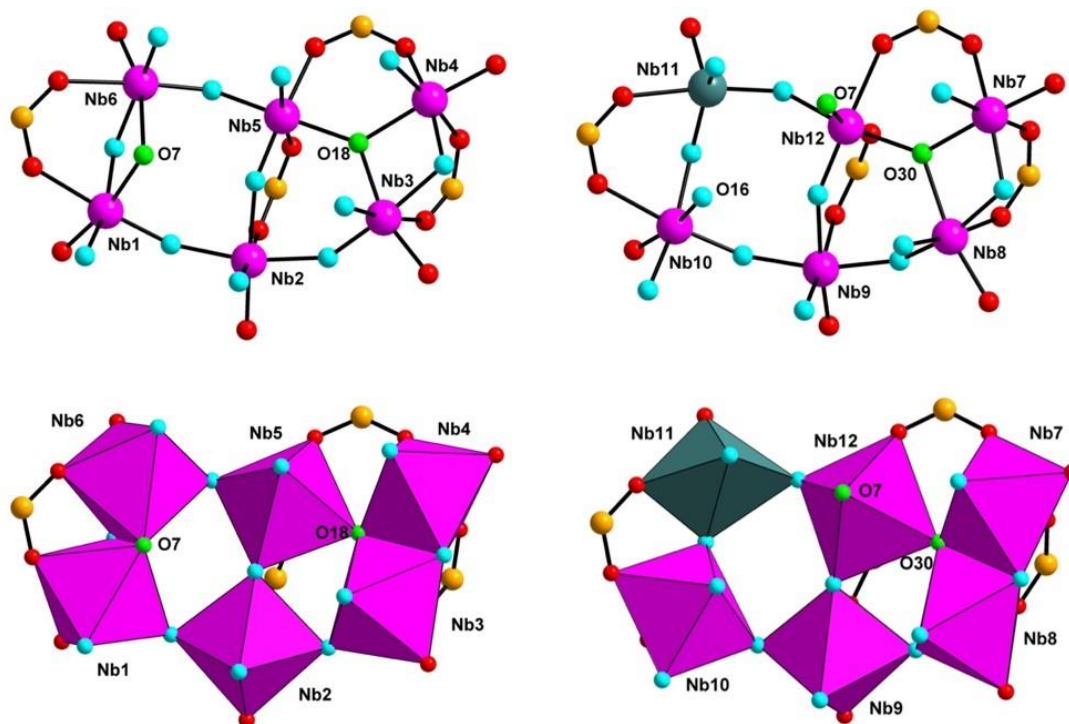


**Figure 1:** Ball and stick (top), and polyhedral (bottom) representation of the two  $\{\text{Nb}_6\}$ -containing subunits A1 (left) and A2 (right) in the molecular  $\{\text{Nb}_{12}\text{O}_{21}\}$  entity A,  $[\text{Nb}_{12}(\mu_3\text{-O})_3(\mu_2\text{-O})_{18}(\text{C}_{15}\text{H}_9\text{O}_2)_8(\text{O}^i\text{Pr})_{10}]$ . Purple circle: Nb centers in octahedral coordination  $[\text{NbO}_6]$ ; dark green circle: Nb11 center in square pyramidal coordination  $[\text{NbO}_5]$ ; green circles:  $\mu_3$ -oxo; cyan circles:  $\mu_2$ -oxo; orange circles: carbon atoms from bidentate carboxylate groups; red circles (bridging): oxygen atoms from carboxylate groups; red circles (terminal): oxygen atoms from isopropanolate species.

The two rectangular-like planes of the  $\{\text{Nb}_6\text{O}_8\}$  (A1) and  $\{\text{Nb}_6\text{O}_7\}$  (A2) subunits are stacked almost perpendicularly, with a tilting angle of around  $104^\circ$ , through seven oxo bridging groups (Figure 2 – top), in order to generate a dodecanuclear moiety  $\{\text{Nb}_{12}\text{O}_{21}\}$ . In this core, there are three oxo groups (O7, O18 & O30) linking three niobium centers ( $\mu_3$  mode) and eighteen oxo groups linking two niobium centers ( $\mu_2$  mode) via corner-sharing fashion. Only three pairs of niobium-centered octahedra are edge-shared, with resulting shorter Nb $\cdots$ Nb distances of 3.1447(13) Å for Nb4 $\cdots$ Nb3, 3.1686(11) Å for Nb7 $\cdots$ Nb8 and 3.2715(11) Å for Nb1 $\cdots$ Nb6. In the case of corner-shared niobium centered octahedra, the Nb $\cdots$ Nb distances are much longer, with values greater than 3.47 Å.



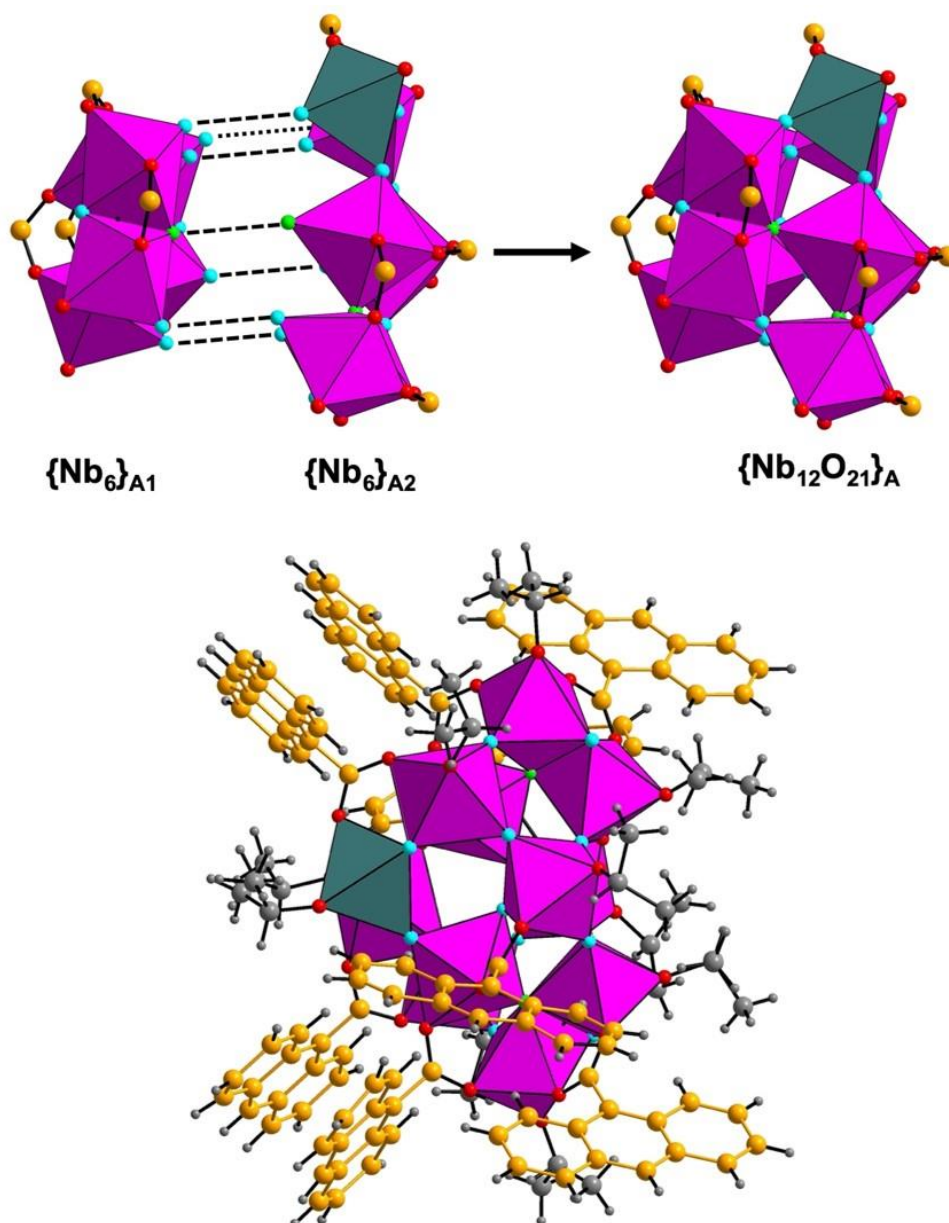


**Figure 2:** (top) Schematic view of the assembly mode of the two {Nb<sub>6</sub>}-containing subunits A1 and A2 in order to construct the {Nb<sub>12</sub>O<sub>21</sub>} oxo cluster of the molecular entity A. The rectangular six membered planes of each {Nb<sub>6</sub>}-containing subunits A1 and A2 are arranged along a tilting angle of around 104°. (bottom) Representation of the {Nb<sub>12</sub>O<sub>21</sub>} oxo cluster (entity A) with surrounding 9-anthracenecarboxylate and isopropanolate species. Purple polyhedra: Nb center in octahedral coordination; dark green polyhedra: Nb center in square pyramidal coordination; green circles:  $\mu_3$ -oxo; cyan circles:  $\mu_2$ -oxo; orange circles: carbon atoms from bidentate carboxylate groups; red circles (bridging): oxygen atoms from carboxylate groups; red circles (terminal): oxygen atoms from isopropanolate species.

The arrangement of niobium-centered polyhedra is almost similar in molecule B, with the construction of two rectangular-like hexameric sub-units B1 & B2 of {Nb<sub>6</sub>O<sub>7</sub>} type, in the same fashion as the previously defined sub-units A2. There exists one pair of edge-sharing octahedrally coordinated niobium atoms, linked via two oxo bridges (one  $\mu_2$  and one  $\mu_3$  types) to a second pair of corner-sharing octahedrally coordinated niobium atoms. The latter is then connected via two oxo bridges (two  $\mu_2$  types) to a third pair of corner-sharing centered-niobium

polyhedra (Figure 3). As found for the sub-unit A2, each hexamer contains one niobium atom (Nb15 & Nb22) exhibiting a square pyramidal environment, with the similar Nb-O<sub>μ2</sub> bond lengths in the range 1.816(13)-1.846(7) Å for Nb15 and 1.842(6)-1.992(13) Å for Nb22, Nb-O<sub>c</sub> bond lengths of 2.155(11) Å (Nb15) and 2.162(10) Å (Nb22), and Nb-O<sub>Pr</sub> bond lengths of 1.811(10) Å (Nb15) and 1.786(10) Å (Nb22). These two niobium centers Nb15 & Nb22 are considered as five-fold coordination since the nearest sixth oxygen atom which would complete the octahedral geometry is very far from the usual Nb-O bond lengths, with values of 2.951(7) Å (for Nb15...O71) and 2.841(7) Å (for Nb22...O58) (see Figure 3 for the location of the O71 & O58 atoms). For the other ten octahedrally coordinated niobium atoms, the Nb-O<sub>μ2/μ3</sub> distances are in the range of 1.792(5)-2.122(5) Å, the Nb-O<sub>c</sub> distances are in the range of 2.083(6)-2.234(8) Å, and the Nb-O<sub>Pr</sub> distances are in the range of 1.833(6)-1.862(6) Å. So, the slight distortion of the Nb6-O7<sub>μ3</sub> bond length (resulting in an octahedral geometry) observed in the hexameric sub-unit A1 does not occur in the sub-units B1 or B2, which both contains one five-fold coordinated niobium atom.

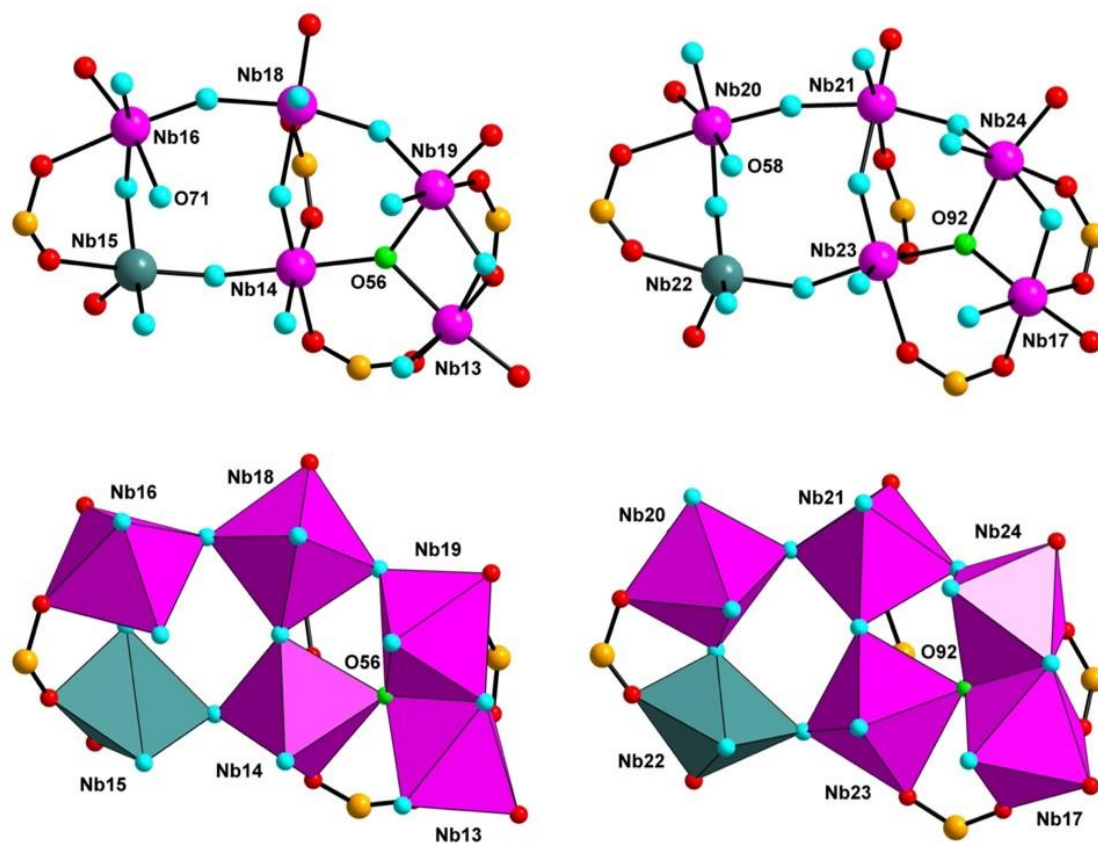


**Figure 3:** Ball and stick (top), and polyhedral (bottom) representation of the two {Nb<sub>6</sub>}-containing subunits B1 (left) and B2 (right) in the molecular {Nb<sub>12</sub>O<sub>21</sub>} entity B, [Nb<sub>12</sub>(μ<sub>3</sub>-O)<sub>2</sub>(μ<sub>2</sub>-O)<sub>19</sub>(C<sub>15</sub>H<sub>9</sub>O<sub>2</sub>)<sub>8</sub>(O<sup>i</sup>Pr)<sub>10</sub>]. Purple circles: Nb centers in octahedral coordination [NbO<sub>6</sub>]; dark green circles: Nb15 & Nb22 centers in square pyramidal coordination [NbO<sub>5</sub>]; green circles: μ<sub>3</sub>-oxo; cyan circles: μ<sub>2</sub>-oxo; orange circles: carbon atoms from bidentate carboxylate groups; red circles (bridging): oxygen atoms from carboxylate groups; red circles (terminal): oxygen atoms from isopropanolate species.

As for molecule A, the two hexanuclear sub-units B1 & B2 of  $\{\text{Nb}_6\text{O}_7\}$  type are connected through seven  $\mu_2$ -oxo groups, giving rise to the formation of a distinct dodecameric core B  $\{\text{Nb}_{12}\text{O}_{21}\}$  (Figure 4 - top). The stacking of these two sub-units B1 & B2 occurs with a tilting angle of around  $110^\circ$ . The B moiety contains two five-coordinated niobium centers, but two  $\mu_3$ -oxo groups and nineteen  $\mu_2$ -oxo groups (instead of three  $\mu_3$ -oxo groups and eighteen  $\mu_2$ -oxo groups in molecule A). The two sets of edge-sharing niobium-centered polyhedra have Nb $\cdots$ Nb distances of 3.1453(11) Å and 3.1555(10) Å for sub-unit B1 and B2, respectively, whereas the Nb $\cdots$ Nb distances involving corner-sharing niobium-centered polyhedral are greater than 4.40 Å.

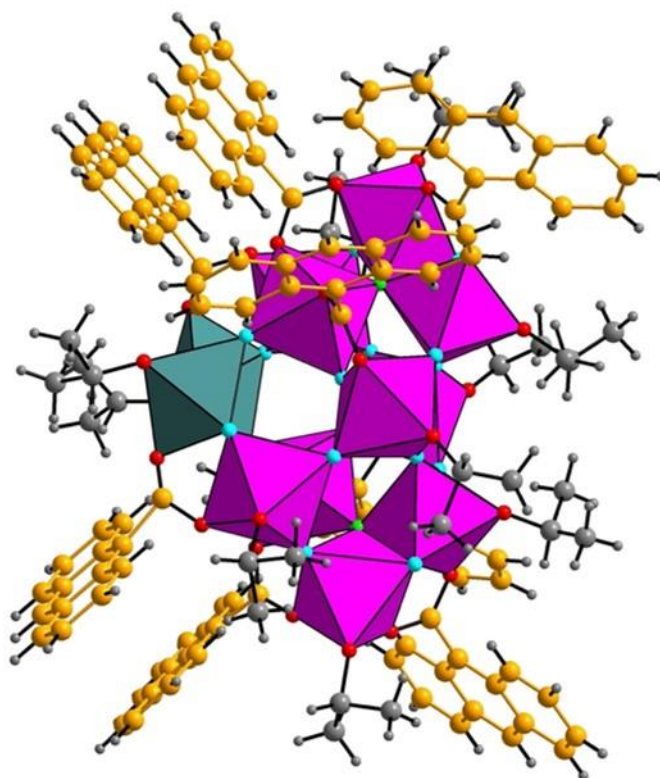
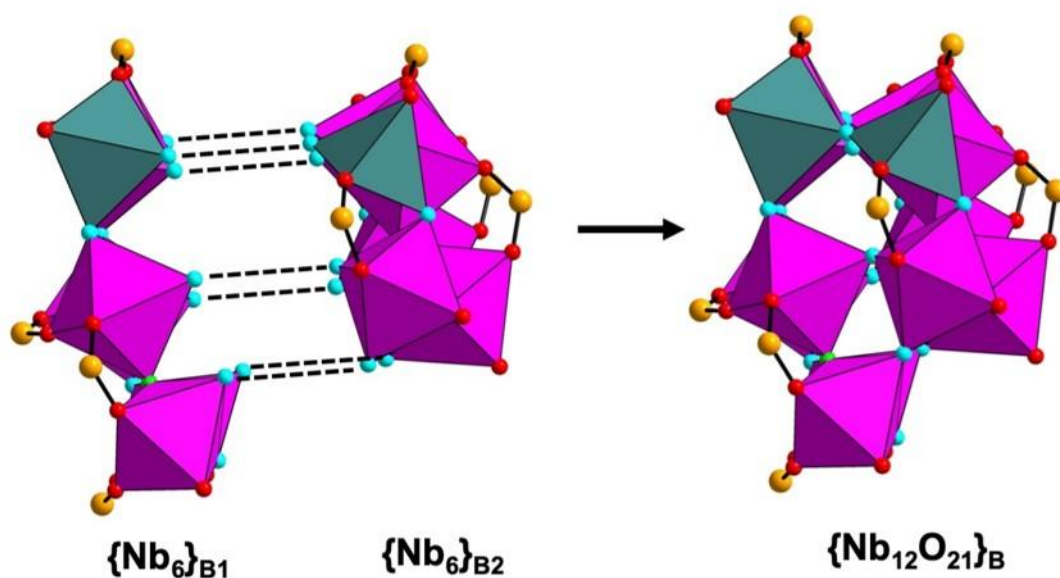


**Figure 4:** (top) Schematic view of the assembly mode of the two  $\{\text{Nb}_6\}$ -containing subunits B1 and B2 in order to construct the  $\{\text{Nb}_{12}\text{O}_{21}\}$  oxo cluster of the molecular entity B. The rectangular six membered planes of each  $\{\text{Nb}_6\}$ -containing subunits B1 and B2 are arranged along a tilting angle of around  $110^\circ$ . (bottom) Representation of the  $\{\text{Nb}_{12}\text{O}_{21}\}$  oxo cluster (entity B) with surrounding 9-anthracenecarboxylate and isopropanolate species. Purple polyhedra: Nb center in octahedral coordination; dark green polyhedra: Nb centers in square pyramidal coordination; green circles:  $\mu_3$ -oxo; cyan circles:  $\mu_2$ -oxo; orange circles: carbon atoms from bidentate carboxylate groups; red circles (bridging): oxygen atoms from carboxylate groups; red circles (terminal): oxygen atoms from isopropanolate species.

Both molecules A & B are decorated by oxygen atoms from ten terminal isopropanolate species and carboxylate arms from eight anthracene-9-carboxylates (Figures 2-bottom and 4-bottom). The carboxylate pincers adopt a *syn-syn* bidentate bridging mode with two neighboring niobium centers. The anthracene-9-carboxylates of A and B entities are interacting to each other through  $\pi$ - $\pi$  stackings between the aromatic rings with typical C $\cdots$ C distances in the range 3.6-3.7 Å. The noticeable point is the occurrence of the five-fold coordination for some niobium centers, which is very uncommon in the poly-oxo niobium(V) carboxylates or poly-oxo niobate clusters.<sup>[13]</sup> Indeed, within the crystal structure, the two molecules A & B only differ by the number of such niobium atoms with square pyramidal geometries, for which apical Nb-O bonding interactions vary from 2.409 Å (sub-unit A1), up to Nb $\cdots$ O of 2.841(7) Å (sub-unit B2), 2.951(7) Å (sub-unit B1) and 3.036(7) Å (sub-unit A2). This metric difference allows to define two asymmetric units with the identical chemical formula of  $\{\text{Nb}_{21}\text{O}_{21}\}$  core. Even if the niobium square pyramidal environment is rarely encountered, it also appears in some dense niobium oxides such as  $\text{Na}_5\text{NbO}_5$ ,<sup>[56]</sup>  $\text{NaKLaNbO}_5$ ,<sup>[57]</sup>  $\text{KLa}_2\text{NbO}_6$ <sup>[58]</sup> or  $\text{Ba}_4\text{Nb}_2\text{O}_9$ .<sup>[59]</sup>

Interestingly, the identification of the  $\{\text{Nb}_{21}\text{O}_{21}\}$  poly-oxo cluster is second type of dodecameric core for the molecular niobium carboxylate family. Indeed, a previous work reported the formation of a dodecanuclear niobium(V) moiety  $\{\text{Nb}_{12}\text{O}_{20}\}$ <sup>[60]</sup> with similar isopropoxy species, but stabilized by means of embonate ligands (from embonic acid – also called pamoic acid), which consist of two 3-hydroxy-2-naphthoate fragments linked through a methylene group. The resulting association of the embonate molecules with niobium(V) gave rise to the isolation of dodecamer, which can be view as the as the stacking of two hexanuclear sub-units composed of three centered niobium atoms in pentagonal bipyramids connected to three peripheral octahedrally coordinated niobium atoms (Figure S4). Apart the similar features of the hexanuclear sub-units, the main difference lies on the variety of coordination environments for niobium, for which there exist mixed 6- and 7-fold environments in  $\{\text{Nb}_{12}\text{O}_{20}\}$  core<sup>[60]</sup> and mixed 5- and 6-fold environments in the present  $\{\text{Nb}_{12}\text{O}_{21}\}$  core.

The analysis of the crystal structure reveals that all the twenty-four crystallographically non-equivalent niobium atoms exhibit a pentavalent oxidation state, as the typical Nb-O bond distance as well as the bond valence calculations (Table S2). Starting from a tetravalent niobium source ( $\text{Nb}^{\text{IV}}\text{Cl}_4(\text{THF})_2$ ), the isolation of such a crystalline compound of  $\{\text{Nb}_{12}\text{O}_{21}\}$  cluster reflects of an oxidation reaction occurring during the synthetical process, and which may explain the very low value of crystallization yield. This might be due to a partial in-situ conversion of niobium(IV) into niobium(V), which gives rise to the formation of  $\{\text{Nb}_{12}\text{O}_{21}\}$ . Considering the synthetic conditions used to for the  $\{\text{Nb}_{12}\text{O}_{21}\}$  cluster, the oxidation process can only be initiated by the small quantity of water formed through the esterification process.

It may also explain why the yield of the reaction is so low. In addition, electronic spectroscopy of the mother liquor after the crystallization process presents a broad transition around 460 nm, that could be attributed to niobium cation under the +IV oxidation state (Figure S5).<sup>[61]</sup>

### **Infrared spectroscopy analysis**

The  $\{\text{Nb}_{12}\text{O}_{21}\}$  compound crystallization process was followed using infrared spectroscopy. Supernatant solutions were collected before crystallization, roughly 1 hour of mixing to homogenize the mixture, and after heating and crystallization of the  $\{\text{Nb}_{12}\text{O}_{21}\}$  compound (after approximately 5 days). On the IR spectrum (Figure 5) of supernatant solutions of the  $\{\text{Nb}_{12}\text{O}_{21}\}$  compound, we can observe several interesting areas. The 3000-2750  $\text{cm}^{-1}$  range is related to the  $\nu(\text{C-H})$  stretching vibrations indicating the presence of the isopropyl groups with the typical asymmetric and symmetric band values at 2970  $\text{cm}^{-1}$  and  $\sim 2882 \text{ cm}^{-1}$ , respectively. The alkoxide ligands are also visible in the 1480-1370  $\text{cm}^{-1}$  region (typical vibrations in the range 1470-1400  $\text{cm}^{-1}$  and at 1373  $\text{cm}^{-1}$ ) which is related to the  $\nu(\text{C-H})$  bending vibrations. The last domain range is between 1200-1000  $\text{cm}^{-1}$  where we observed the  $\nu(\text{C-O})$  vibrations of linked isopropoxide ligand at characteristic peaks located at 1096 and 1057  $\text{cm}^{-1}$ . The last broad vibrations in the molecule fingerprint at 529  $\text{cm}^{-1}$  are related to the  $\nu(\text{Nb-O})$  stretching mode. All these vibrations are visible for the supernatant solutions as well as the crystallized compound and the niobium ethoxide precursor.

The other interesting point is related to the formation of the  $\{\text{Nb}_{12}\text{O}_{21}\}$  compound. For this purpose, we can focus on the free ligand and compound spectra and see that the  $\nu(\text{C=O})$  vibration of the free carboxylic acid function of the anthracene ligand located at 1678  $\text{cm}^{-1}$  disappears to the advantage of those of bonded carboxylate arm,  $\nu_{\text{asym}}(\text{COO})$  and  $\nu_{\text{sym}}(\text{COO})$  centered at 1624 and 1538  $\text{cm}^{-1}$  in the spectrum of the crystalline compound. Furthermore, the  $\nu(\text{C}_{\text{arom-H}})$  vibrations of the anthracene ligands are also visible on both spectra above 3000  $\text{cm}^{-1}$ . The formation of an ester due to the esterification mentioned earlier could be confirmed by the presence of vibration in the range 1710 – 1695  $\text{cm}^{-1}$ . They appear to be extremely weak in this case and are not always observed in this kind of mixtures. <sup>[51]</sup>

However, there is no evidence of the presence of the  $\{\text{Nb}_{12}\}$  compound in the supernatant solutions. The  $\nu(\text{C=O})$  and  $\nu(\text{COO})$  vibrations are summarized in Table 2.

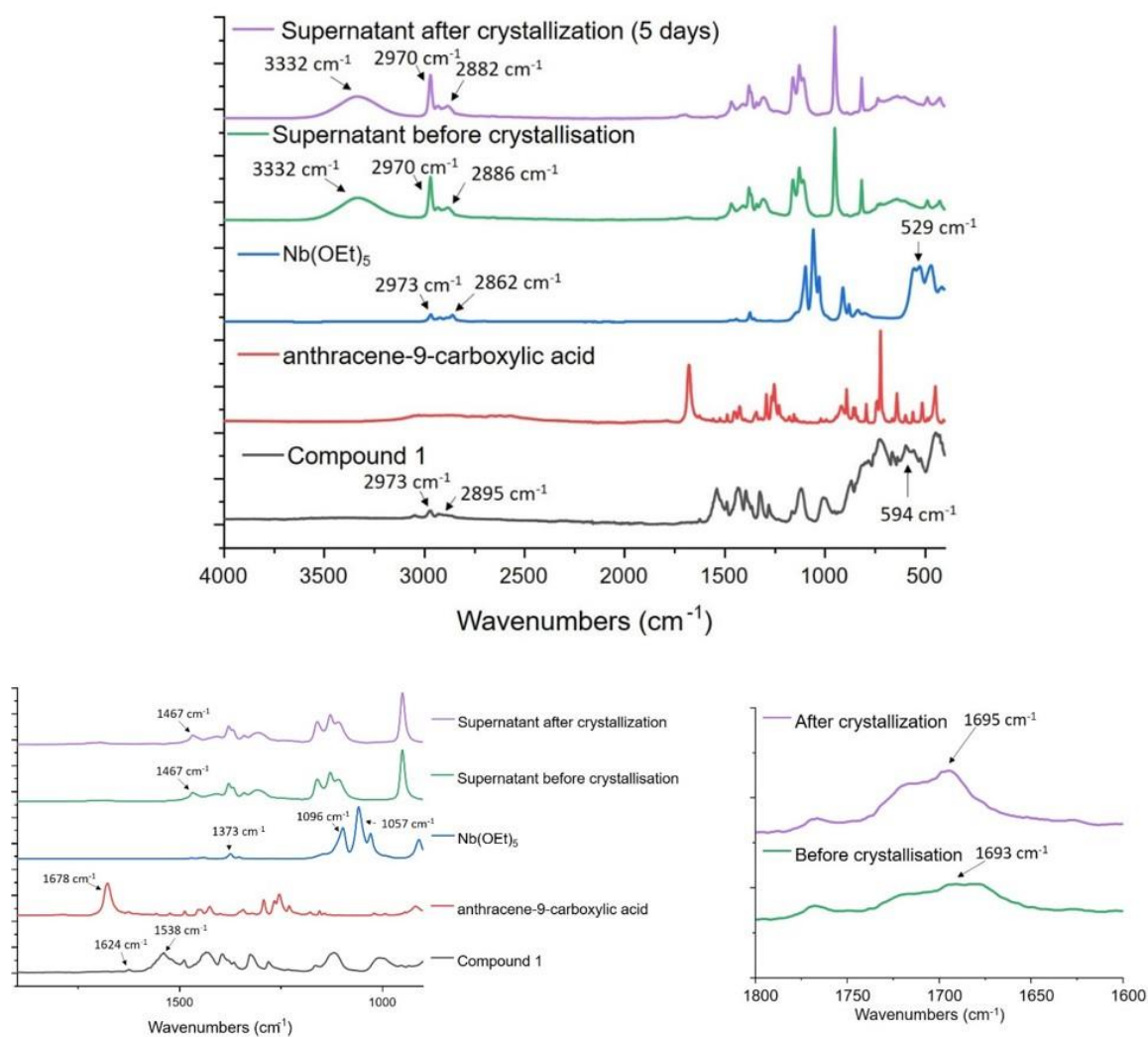


**Fig. 5.** Infrared spectroscopy analysis for compound  $\{\text{Nb}_{12}\text{O}_{21}\}$ . Infrared spectra of  $\text{Nb}(\text{OEt})_5$  (blue line), anthracene-9-dicarboxylic acid (red line), supernatant after 1h mixing at room temperature (green line), supernatant after crystallization (purple line) and compound  $\{\text{Nb}_{12}\text{O}_{21}\}$  (black line). Top: full spectrum in the 4000-400  $\text{cm}^{-1}$  range; bottom left: detailed region in the 950-1900  $\text{cm}^{-1}$  range; bottom right: detailed region in the 1800-1600  $\text{cm}^{-1}$  range.

**Table 2.** Attribution of the  $\nu(\text{C}=\text{O})$  vibrations (from carboxylic acid function) and  $\nu(\text{COO})$  vibrations (from carboxylate function) for compound  $\{\text{Nb}_{12}\text{O}_{21}\}$  (in  $\text{cm}^{-1}$ ).

		$\nu(\text{C}=\text{O})_{\text{acid}}$	$\nu_{\text{asym}}(\text{COO})$	$\nu_{\text{sym}}(\text{COO})$
	Anthracene-9-carboxylic acid	1678	/	/
$\{\text{Nb}_{12}\text{O}_{21}\}$	Supernatant (1 hour)	/	n.o. [a]	n.o. [a]
	Supernatant (5 days)	/	n.o. [a]	n.o. [a]
	Crystalline product	/	1624	1538

### MAS $^{93}\text{Nb}$ NMR spectrum

Compound  $\{\text{Nb}_{12}\text{O}_{21}\}$  can be considered as a high nuclearity niobium cluster which involves two different  $\{\text{Nb}_{12}\}$  cores, not as symmetrical as other ones reported.<sup>[50]</sup> Nevertheless, the fact that it contains two different coordination sites makes  $\{\text{Nb}_{12}\text{O}_{21}\}$  an interesting compound for recording an NMR spectrum. We have first tried to measure a spectrum using liquid NMR

without success due to the insolubility of the compound despite the use of several deuterated solvents (DMF, DMSO,  $\text{CDCl}_3$ , EtOD, MeOD). Consequently, we turn towards solid-state NMR. A MAS  $^{93}\text{Nb}$  NMR spectrum was recorded at high magnetic field (18.8 T) and under MAS (magic-angle spinning, Figure 6). The ultra-wideline observed suggests an overlapping of different peaks that could not be resolved with the MAS. Such overlapping precludes an accurate fitting of the quadrupolar parameters but the maximum peak position is observed at -680 ppm, which is in line with the range of the chemical shift of 6-fold environment of the niobium(V).<sup>[62]</sup> Another signal is detected at -360 ppm deshielded compared to the main peak. The  $^{93}\text{Nb}$  chemical shifts are known to be sensitive to the coordination number of the niobium,<sup>[62]</sup> and this signal may be attributed to the five-coordinated niobium. This conclusion is also supported by the other characterization methods of this article.

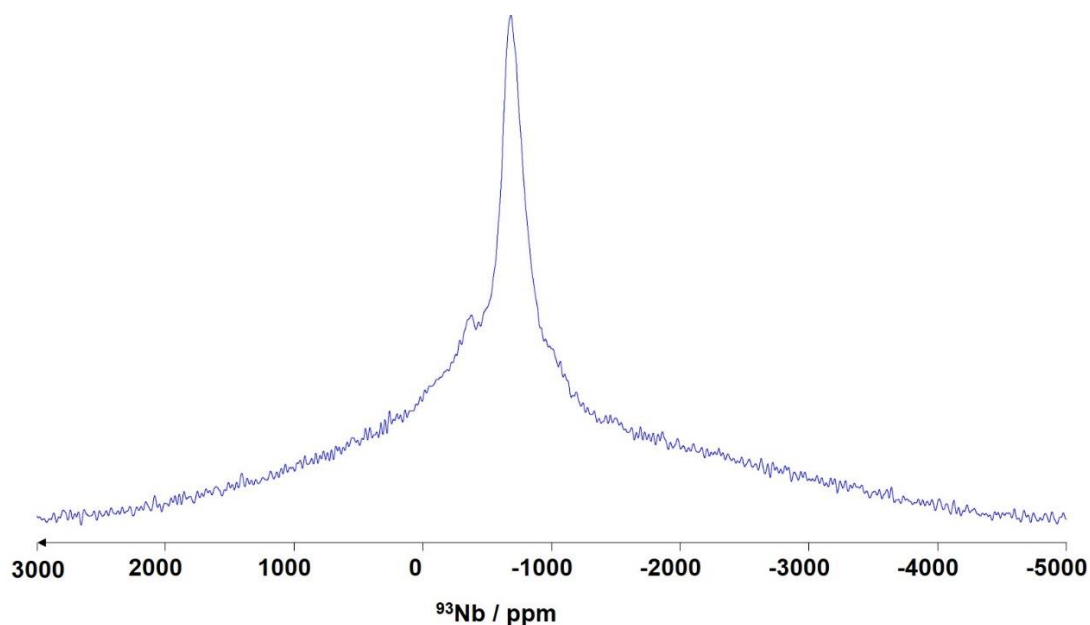


**Fig. 6.** MAS NMR  $^{93}\text{Nb}$  spectrum of compound  $\{\text{Nb}_{12}\text{O}_{21}\}$  recorded at 18.8 T and  $\nu_0 = 62.5$  kHz.

## Conclusion

In summary, the reactivity of tetravalent niobium (under the pristine form  $\text{NbCl}_4 \cdot 2\text{THF}$ ) with the anthracene-9-carboxylate ligand leads to the formation and crystallization of an unprecedented compound containing two dodecanuclear  $\{\text{Nb}_{12}\text{O}_{21}\}$  niobium(V) cores stabilized by anthracene-9-carboxylate and isopropanolates ligands. This polynuclear entity constitutes a second illustration with twelve niobium-oxo centers complexed by carboxylate ligands, involved in the  $\{\text{Nb}_{12}\text{O}_{21}\}$  together with the one stabilized by embonate ligands constituted of a  $\{\text{Nb}_{12}\text{O}_{20}\}$  moieties.<sup>[60]</sup> Single crystal X-ray diffraction reveals the presence of rare 5-fold coordinated niobium(V) centers with a distorted square pyramidal geometry and more classical 6-fold coordinated niobium(V) with octahedral geometries. MAS  $^{93}\text{Nb}$  NMR spectrum suggest the presence of the 6-fold coordinated niobium(V) but despite their presence, the 5-fold coordinated niobium(V) centers were not clearly observed, possibly due to the overlapping by the large pic attributed to the octahedral niobium cations. Further work will

focus in the comprehension about the formation of such large hybrid niobium cluster using monotopic carboxylic ligands, since the largest reported polynuclear moiety is currently the  $\{\text{Nb}_{16}\text{O}_{28}\}^{[49]}$ . This opens new prospects to discover molecular systems with high nuclearity when compared with the wide variety and range of polyoxoniobates occurring with niobyl species.<sup>[13]</sup>

## Experimental Section

**Reagents.** The following reactants were used: niobium(IV)chloride ( $\text{Nb}(\text{OCH}_2\text{CH}_3)_5$ , 99.95%, Sigma-Aldrich), anthracene-9-carboxylic acid ( $\text{C}_{15}\text{H}_{10}\text{O}_2$ , 99% Sigma-Aldrich), anhydrous isopropanol ( $\text{C}_3\text{H}_8\text{O}$ ,  $\text{HO}^i\text{Pr}$ , 99.5%, Sigma-Aldrich). The chemical reactants were commercially available, were used without any further purification and manipulated in a glove box under argon to prevent any hydrolysis reaction of the niobium(IV) into niobium(IV or V)oxide.

### Syntheses

**Compound**  $[[\text{Nb}_{12}(\mu_3\text{-O})_3(\mu_2\text{-O})_{18}(\text{C}_{15}\text{H}_9\text{O}_2)_8(\text{O}^i\text{Pr})_{10}]\cdot[\text{Nb}_{12}(\mu_3\text{-O})_2(\mu_2\text{-O})_{19}(\text{C}_{15}\text{H}_9\text{O}_2)_8(\text{O}^i\text{Pr})_{10}]\cdot\approx 7(\text{HO}^i\text{Pr})$  (called  $\{\text{Nb}_{12}\text{O}_{21}\}$ ): A mixture of 12 mg (0.05 mmol)  $\text{NbCl}_4(\text{THF})_2$ , 50 mg (0.23 mmol) anthracene-9-carboxylic acid and isopropanol (1 mL, 13.1 mmol) was placed in a 2 mL glass tube, sealed with a phenolic cap, and placed in an oven at 120 °C. After 5 days orange parallelepiped blocks appeared. Compound  $\{\text{Nb}_{12}\text{O}_{21}\}$  was analyzed by optical microscope showing large parallelepiped-shape crystals up to 100  $\mu\text{m}$  size, which are suitable for further SCXRD analyses (Figure S1). The resulting orange crystals filtered off, washed with isopropanol and dried at room temperature. Crystallization yield was 4.2 %Nb. Crystals of compound  $\{\text{Nb}_{12}\text{O}_{21}\}$  were found to be stable under air for several weeks and manipulated under ambient air, without any specific precaution.

### Single-crystal X-ray diffraction

X rays diffraction intensities of crystals of compound  $\{\text{Nb}_{12}\text{O}_{21}\}$  was collected from a synchrotron radiation facility (PROXIMA-2 A beamline, SOLEIL, France) by using a wavelength of  $\lambda = 0.7293 \text{ \AA}$  at 100 K (under liquid nitrogen gas flow). The structural analysis shows high values for many thermal parameters related to the organic ligands. Due to this observation, most of the anthracenoate ligands were modelled using a rigid body approach. The aromatic part of the ligands was constructed and added to the model and refined by constraining the carbon atoms positions. Some restraints (DFIX, DANG and SIMU) were used on some isopropanolate ligands to stabilize the C-C and C-O distances that were heavily moving due to the high values for the thermal parameters of the carbon and oxygen atoms. The metal-oxo part of the compound was refined classically by successful difference Fourier syntheses, and refined by full-matrix least-squares on all  $F^2$  data using SHELX program suites, implemented in the OLEX2 graphical tool.<sup>[63]</sup>



Data reduction was accomplished using SAINT V8.34a.<sup>[64]</sup> The substantial redundancy in data allowed a semi-empirical absorption correction (SADABS V2014/5) to be applied, on the basis of multiple measurements of equivalent reflections.<sup>[65]</sup>

The crystal data are given in Table 1. Supporting information is available in CIF format. CCDC numbers: 2280853 for **1**, contain the supplementary crystallographic data for this paper. These data can be obtained free of charge from The Cambridge Crystallographic Data Centre via [www.ccdc.cam.ac.uk/data\\_request/cif](http://www.ccdc.cam.ac.uk/data_request/cif).

**Table 1.** Crystal data and structure refinements for {Nb<sub>12</sub>O<sub>21</sub>} compound.

	{Nb <sub>12</sub> O <sub>21</sub> }
Formula	C <sub>300</sub> H <sub>284</sub> Nb <sub>24</sub> O <sub>94</sub>
Formula weight	7323.09
Temperature/K	100
Crystal type	orange parallelepiped
Crystal size/mm	0.04 x 0.015 x 0.015
Crystal system	triclinic
Space group	<i>P</i> -1
<i>a</i> /Å	18.9105(8)
<i>b</i> /Å	30.3622(13)
<i>c</i> /Å	31.0424(14)
<i>α</i> /°	111.3772(16)
<i>β</i> /°	97.6406(17)
<i>γ</i> /°	103.9729(17)
Volume/Å <sup>3</sup>	15617.1(12)
<i>Z</i> , ρ <sub>calculated</sub> /g.cm <sup>-3</sup>	2, 1.621
μ/mm <sup>-1</sup>	0.993
θ range/°	0.75 - 22.50
Limiting indices	-22 ≤ <i>h</i> ≤ 22 -33 ≤ <i>k</i> ≤ 33 -32 ≤ <i>l</i> ≤ 34
Collected reflections	150210
Unique reflections	47641 [R(int) = 0.0409]
Parameters	3443
Goodness-of-fit on F <sup>2</sup>	1.084
Final R indices [I > 2σ(I)]	R1 = 0.0772 wR2 = 0.2555
R indices (all data)	R1 = 0.0881 wR2 = 0.2699
Largest diff. peak and hole/e.Å <sup>-3</sup>	1.608 and -1.452

### Powder X-ray diffraction

X-ray powder diffraction was performed on Bruker D8 Advance diffractometer (LynxEye detector) in a Bragg-Brentano  $\theta$ - $\theta$  mode using Cu-K $\alpha$  radiation. Each powder pattern was recorded by using a classical glass specimen holder, within an angular range of 5-50° in  $2\theta$ , with steps of 0.02° and counting time of 0.5 s per step.

### Infrared spectroscopy

Infrared spectrum was measured on Perkin Elmer Spectrum Two<sup>TM</sup> spectrometer between 4000 and 400 cm<sup>-1</sup>, equipped with a diamond Attenuated Total Reflectance (ATR) accessory. No ATR correction was applied on the spectrum.

### **MAS $^{93}\text{Nb}$ NMR spectroscopy**

$^{93}\text{Nb}$  NMR spectra were recorded at 18.8 T (800 MHz for  $^1\text{H}$ ) using a narrow-bore Bruker BioSpsin spectrometer equipped with an AVANCE-III console and a 1.3 mm HX probe with a spinning speed of 62.5 kHz. A rotor synchronized solid echo (90- $\tau$ -90 with  $\tau$  corresponding to one rotor period) was used with a pulse length of 4.5  $\mu\text{s}$ , a radiofrequency field amplitude of 55 kHz and a recycle delay of 0.25 s. The spectrum is the sum of 68752 scans.  $^{93}\text{Nb}$  chemical shifts were externally referenced to  $\text{NbCl}_5$  (1 mol/L) at 0 ppm.

### **Acknowledgements**

The authors would like to thank Mrs. Nora Djelal, Laurence Burylo and Philippe Devaux for their assistances with the synthesis, XRD powder patterns measurements (UCCS). Dr Clément Falaise (Université of Versailles Saint Quentin-en-Yvelines) is thanked for his help in the single-crystal XRD data collection (compound **1**) at synchrotron SOLEIL (France). The "Fonds Européen de Développement Régional (FEDER)", "CNRS", "Région Hauts de France" and "Ministère de l'Education Nationale de l'Enseignement Supérieur et de la Recherche" are acknowledged for the funding of X-ray diffractometers from the Chevreul Institute platform.

### **Keywords**

coordination complex, niobium(V), MAS  $^{93}\text{Nb}$  NMR, poly-oxo clusters, single-crystal X-ray diffraction.

### **Conflict of Interests**

The authors declare no conflict of interest.

### **Data Availability Statement**

Supporting Information for this article is available on the WWW under <https://doi.org/10.1002/chem.2022XXX>.

The data associated with the findings of this study can be found in the online version (optical microscope photographs, powder XRD pattern, IR spectra, liquid  $^1\text{H}$  NMR and solid state  $^{93}\text{Nb}$  spectra, summary of the representation of polynuclear niobium-centered cores).

### **Accession Codes**

Crystallographic data for the structural analysis has been deposited with the Cambridge Crystallographic Data Centre, CCDC No. 2280853 for **1**. Copies of the data can be obtained free of charge on application to CCDC, 12 Union Road, Cambridge CB2 1EZ (fax: +44-1223-336-033; e-mail: [data\\_request@ccdc.cam.ac.uk](mailto:data_request@ccdc.cam.ac.uk)).

## References

- [1] I. Nowak, M. Ziolk, *Chem. Rev.* **1999**, *99*, 3603–3624.
- [2] A. G. S. Prado, L. B. Bolzon, C. P. Pedrosa, A. O. Moura, L. L. Costa, *Appl. Catal. B: Environ.* **2008**, *82*, 219–224.
- [3] K. Tanabe, S. Okazaki, *Appl. Catal. A: Gen.* **1995**, *133*, 191–218.
- [4] B. M. Weckhuysen, D. E. Keller, *Catal. Today* **2003**, *78*, 25–46.
- [5] K. Tanabe, *Catal. Today* **2003**, *78*, 65–77.
- [6] K. Tanabe, *Mater. Chem. Phys.* **1987**, *17*, 217–225.
- [7] F. A. Cotton, M. P. Diebold, W. J. Roth, *Inorg. Chem.* **1987**, *26*, 2889–2893.
- [8] P. B. Arimondo, F. Calderazzo, U. Englert, C. Maichle-Mössmer, G. Pampaloni, J. Strähle, *J. Chem. Soc., Dalton Trans.* **1996**, 311–319.
- [9] B.-L. Ooi, Q. Xu, T. Shibahara, *Inorg. Chim. Acta* **1998**, *274*, 103–107.
- [10] B.-L. Ooi, G. Sakane, T. Shibahara, *Inorg. Chem.* **1996**, *35*, 7452–7454.
- [11] A. Antiñolo, S. García-Yuste, I. López-Solera, A. Otero, J. C. Pérez-Flores, I. D. Hierro, L. Salvi, H. Cattey, Y. Mugnier, *J. Organomet. Chem.* **2005**, *690*, 3134–3141.
- [12] B.-L. Ooi, I. Søjtofte, J. J. Vittal, *Inorg. Chim. Acta* **2004**, *357*, 625–629.
- [13] H.-Y. Zhao, Y.-Z. Li, J.-W. Zhao, L. Wang, G.-Y. Yang, *Coord. Chem. Rev.* **2021**, *443*, 213966.
- [14] I. Lindqvist, *Ark. Kemi.* **1952**, *5*, 247–250.
- [15] Y. Wu, X. Li, Y. Qi, H. Yu, L. Jin, S. Zheng, *Angew. Chem. Int. Ed.* **2018**, *57*, 8572–8576.
- [16] N. Galešić, N. Brničević, B. Matković, M. Herceg, B. Zelenko, M. Šljukić, B. Prelesnik, R. Herak, *J. Less Common Met.* **1977**, *51*, 259–270.
- [17] L. Eriksson, G. Svensson, V. Tabachenko, J. Sjöblom, T. K. Thorsen, P. Coppens, O. Buchardt, *Acta Chem. Scandi.* **1993**, *47*, 1038–1040.
- [18] B. Kojić-Prodić, R. Liminga, S. Ščavaničar, *Acta Crystallogr B Struct Sci* **1973**, *29*, 864–869.
- [19] G. Mathern, R. Weiss, *Acta Crystallogr. B Struct. Crystallogr. Cryst. Chem.* **1971**, *27*, 1610–1618.
- [20] M. Šestan, B. Perić, G. Giester, P. Planinić, N. Brničević, *Struct. Chem.* **2005**, *16*, 409–414.
- [21] A. A. Shmakova, E. M. Glebov, V. V. Korolev, D. V. Stass, E. Benassi, P. A. Abramov, M. N. Sokolov, *Dalton Trans.* **2018**, *47*, 2247–2255.
- [22] M. Jurić, P. Planinić, N. Brničević, D. Matković-Čalogović, *J. Mol. Struct.* **2008**, *888*, 266–276.
- [23] W. X. C. Oliveira, C. L. M. Pereira, C. B. Pinheiro, K. Krambrock, T. Grancha, N. Moliner, F. Lloret, M. Julve, *Polyhedron* **2016**, *117*, 710–717.
- [24] M. Jurić, B. Perić, N. Brničević, P. Planinić, D. Pajić, K. Zadro, G. Giester, B. Kaitner, *Dalton Trans.* **2008**, 742–754.
- [25] C. N. Muniz, H. Patel, D. B. Fast, L. E. S. Rohwer, E. W. Reinheimer, M. Dolgos, M. W. Graham, M. Nyman, *J. Solid State Chem.* **2018**, *259*, 48–56.
- [26] M. Jurić, J. Popović, A. Šantić, K. Molčanov, N. Brničević, P. Planinić, *Inorg. Chem.* **2013**, *52*, 1832–1842.

- [27] D. Bayot, B. Tinant, M. Devillers, *Catal. Today* **2003**, 78, 439–447.
- [28] D. Bayot, B. Tinant, B. Mathieu, J. Declercq, M. Devillers, *Eur. J. Inorg. Chem.* **2003**, 2003, 737–743.
- [29] D. Bayot, B. Tinant, M. Devillers, *Inorg. Chem.* **2005**, 44, 1554–1562.
- [30] D. A. Brown, M. G. H. Wallbridge, N. W. Alcock, *J. Chem. Soc., Dalton Trans.* **1993**, 2037.
- [31] D. A. Brown, M. G. H. Wallbridge, W. S. Li, M. McPartlin, I. J. Scowen, *Inorganica Chimica Acta* **1994**, 227, 99–104.
- [32] D. A. Brown, M. G. H. Wallbridge, W. S. Li, M. McPartlin, *Polyhedron* **1994**, 13, 2265–2270.
- [33] D. A. Brown, M. G. H. Wallbridge, N. W. Alcock, *J. Chem. Soc., Dalton Trans.* **1993**, 2037–2039.
- [34] D. C. Bradley, R. C. Mehrotra, I. P. Rothwell, A. Singh, *Alkoxo and Aryloxo Derivatives of Metals*, **2001**.
- [35] D. C. Bradley, *Chem. Rev.* **1989**, 89, 1317–1322.
- [36] D. C. Bradley, R. C. Mehrotra, D. P. Gaur, *Metal Alkoxides*, Academic Press, United Kingdom, **1978**.
- [37] C. D. Chandler, Christophe. Roger, M. J. Hampden-Smith, *Chemical Reviews* **1993**, 93, 1205–1241.
- [38] I. Gautier-Luneau, A. Mosset, J. Galy, *Z. Kristallogr. Cryst. Mater.* **1987**, 180, 83–96.
- [39] S. Doeuff, Y. Dromzee, F. Taulelle, C. Sanchez, *Inorg. Chem.* **1989**, 28, 4439–4445.
- [40] T. J. Boyle, R. P. Tyner, T. M. Alam, B. L. Scott, J. W. Ziller, B. G. Potter, *J. Am. Chem. Soc.* **1999**, 121, 12104–12112.
- [41] T. J. Boyle, T. M. Alam, C. J. Tafoya, B. L. Scott, *Inorg. Chem.* **1998**, 37, 5588–5594.
- [42] U. Schubert, E. Arpac, W. Glaubitt, A. Helmerich, C. Chau, *Chem. Mater.* **1992**, 4, 291–295.
- [43] D. J. Eichorst, K. E. Howard, D. A. Payne, S. R. Wilson, *Inorg. Chem.* **1990**, 29, 1458–1459.
- [44] N. Steunou, C. Bonhomme, C. Sanchez, J. Vaissermann, L. G. Hubert-Pfalzgraf, *Inorg. Chem.* **1998**, 37, 901–910.
- [45] L. G. Hubert-Pfalzgraf, V. Abada, S. Halut, J. Roziere, *Polyhedron* **1997**, 16, 581–585.
- [46] T. J. Boyle, T. M. Alam, D. Dimos, G. J. Moore, C. D. Buchheit, H. N. Al-Shareef, E. R. Mechenbier, B. R. Bear, J. W. Ziller, *Chem. Mater.* **1997**, 9, 3187–3198.
- [47] J. H. Thurston, K. H. Whitmire, *Inorg. Chem.* **2003**, 42, 2014–2023.
- [48] P. A. Abramov, M. N. Sokolov, *Molecules* **2023**, 28, 4912.
- [49] M. D. Korzyński, L. S. Xie, M. Dincă, *Helvetica Chimica Acta* **2020**, 103, e2000186.
- [50] D. Andriotou, S. Duval, C. Volkringer, X. Trivelli, W. E. Shepard, T. Loiseau, *Chem. Eur. J.* **2022**, 28, e202201464.
- [51] D. Andriotou, S. Duval, X. Trivelli, C. Volkringer, T. Loiseau, *CrystEngComm* **2022**, 24, 5938–5948.
- [52] D. Andriotou, S. Duval, C. Volkringer, A. M. Arevalo-Lopez, P. Simon, H. Vezin, T. Loiseau, *Inorg. Chem.* **2022**, 61, 15346–15358.
- [53] J. P. Cummings, S. H. Simonsen, *Am. Mineral.* **1970**, 55, 90–97.

- [54] V. Thangadurai, P. Schmid-Beurmann, W. Weppner, *J. Solid State Chem.* **2001**, *158*, 279–289.
- [55] S. Surblé, S. Obbade, S. Saad, S. Yagoubi, C. Dion, F. Abraham, *J. Solid State Chem.* **2006**, *179*, 3238–3251.
- [56] E. Kleinpeter, S. Behrendt, L. Beyer, *Z. Anorg. Allg. Chem.* **1982**, *495*, 105–114.
- [57] J.-H. Liao, M.-C. Tsai, *Cryst. Growth Des.* **2002**, *2*, 83–85.
- [58] I. P. Roof, S. Park, T. Vogt, V. Rassolov, M. D. Smith, S. Omar, J. Nino, *Chem. Mater.* **2008**, *20*, 3327–3335.
- [59] M. T. Dunstan, F. Blanc, M. Avdeev, G. J. McIntyre, C. P. Grey, C. D. Ling, *Chem. Mater.* **2013**, *25*, 3154–3161.
- [60] L.-B. Yuan, Y.-P. He, L. Zhang, J. Zhang, *Inorg. Chem.* **2018**, *57*, 4226–4229.
- [61] Bee-Lean Ooi, T. Shihabara, G. Sakane, Kum-Fun Mok, *Inorg. Chim. Acta* **1997**, *266*, 103–107.
- [62] O. B. Lapina, D. F. Khabibulin, K. V. Romanenko, Z. Gan, M. G. Zuev, V. N. Krasil'nikov, V. E. Fedorov, *Solid State Nucl. Magn. Reson.* **2005**, *28*, 204–224.
- [63] O. V. Dolomanov, L. J. Bourhis, R. J. Gildea, J. A. K. Howard, H. Puschmann, *J. Appl. Crystallogr.* **2009**, *42*, 339–341.
- [64] *Brucker Analytical X-ray Systems: Madison, WI, 2008* **2014**.
- [65] G. M. Sheldrick, *Brucker-Siemens Area detector Absorption and Other Correction* **2015**.